

## RESEARCH ARTICLE



### OPEN ACCESS

Received: 23-01-2023

Accepted: 09-06-2023

Published: 13-09-2023

**Citation:** Lalduhawma K, Vanthangliana V, Bharali B, Kumar S, Bawri GR (2023) Depositional Environment and Diagenetic Process of Bhuban Sandstone: Constraints from the Petrographic Characteristics. Indian Journal of Science and Technology 16(SP1): 208-218. <https://doi.org/10.17485/IJST/v16sp1.msc28>

\* **Corresponding author.**

[vantea\\_g@yahoo.com](mailto:vantea_g@yahoo.com)

**Funding:** None

**Competing Interests:** None

**Copyright:** © 2023 Lalduhawma et al. This is an open access article distributed under the terms of the [Creative Commons Attribution License](https://creativecommons.org/licenses/by/4.0/), which permits unrestricted use, distribution, and reproduction in any medium, provided the original author and source are credited.

Published By Indian Society for Education and Environment ([iSee](https://www.indjst.org/))

**ISSN**

Print: 0974-6846

Electronic: 0974-5645

## Depositional Environment and Diagenetic Process of Bhuban Sandstone: Constraints from the Petrographic Characteristics

K Lalduhawma<sup>1</sup>, V Vanthangliana<sup>2\*</sup>, Bubul Bharali<sup>2</sup>, Shiva Kumar<sup>3</sup>, Gautam Raj Bawri<sup>3</sup>

<sup>1</sup> Dept. of Geology, Lunglei Govt. College, Lunglei, Mizoram, India

<sup>2</sup> Dept. of Geology, Pachhunga University College, Aizawl, Mizoram, India

<sup>3</sup> Dept. of Geology, Mizoram University, Aizawl, Mizoram, India

### Abstract

**Objectives:** The present investigation focuses mainly on the depositional environment and diagenetic processes of Bhuban sandstone using petrographical investigation in and around Lunglei town. **Methods:** A comprehensive field investigation was carried out to investigate the lithofacies variation and thin section examination of the Bhuban Sandstones. A total of 37 representative rock samples were collected during fieldwork from different localities in and around Lunglei Town. Leica DME2700 P petrological microscope with Leica DFC420 camera and Leica Image Analysis software (LAS-v4.6) installed at the Department of Geology, Mizoram University, was used to conduct petrographic and modal analysis. **Findings:** Petrographic analysis of thin sections show that the grains are fine to medium, moderately sorted, and have sub-angular to sub-rounded shape. According to the petrographic plots and thin section studies, the majority of the rocks are Sublitharenite with a little amount of Sub Arkose. The sediments may have originated from a continental orogen-type source and were deposited in a shallow marine environment. The plutonic sources with some upper to lower-rank metamorphics constituted the majority of the sediments. Additionally, prior to deposition, the sediments underwent a modest amount of weathering due to the humid climate. The study also reveals straight, concavo-convex, and suture contact, frequently deformed micas conforming to the grain boundary of quartz, and common flowage of clay minerals along the pores of the grain suggesting a high degree of compaction. In addition, the dissolution of quartz, potash feldspar, and plagioclase feldspar subsequently replaced by other minerals suggested a mesogenesis to telogenesis for the events of diagenesis of the Bhuban sandstones of the study area. **Novelty:** Based on petrographical studies, Bhuban sandstones are derived from plutonic sources with a moderate degree of weathering and deposited in an active continental margin setting. Moreover, the sandstones in the study area underwent a high degree of compaction.

**Keywords:** Surma Basin; Bhuban sandstone; Diagenesis; Lunglei; Quartz; Sublitharenite

---

## 1 Introduction

Surma Basin, the southern extension of Indo-Burmese Ranges witnessed a thick accumulation of Tertiary Sediments, which deformed to develop an N-S trending hill ranges as a collisional result between the Indian and Burmese plate. The majority of Miocene sediments (Surma Group) are well developed and exposed in most parts of the Surma Basin, while Oligocene sediments (Barail Group) are exposed at the eastern margin of the basin and also formed a base for the deposition of Miocene sedimentation. Sporadic occurrences of fluvial sediments (Tipam Group) are exposed at the western margin of Surma Basin. The source rock of the area and the tectonic settings of the sedimentary basins are revealed by the petrography of sedimentary rocks. In Mizoram, many workers have conducted a number of geological investigations. According to the geochemical and petrographic features of the Muthi sandstones of the Upper Bhuban Formation, the rock is litharenite<sup>(1)</sup>. According to Lalnunmawia and Lalhlipuii<sup>(2)</sup> petrographic modal analysis, the sandstones are sublitharenite to litharenite with recycled orogeny origins. Bharali<sup>(3)</sup> mentioned that Bhuban sandstones are sublith-arenite, lithic-wacke, and feldspathic-litharenite types which have been sourced from granitoid and middle to upper-rank metamorphic. Based on this study, it reveals that the maturity of the sediments is significantly high with more recycling of sediments supplied from continental block provenance which has moderate nature of weathering under humid to subhumid climatic conditions. Although central and some of the eastern parts of the basin have been studied by researchers, most of the other parts still need more study to understand the various basinal aspects. Therefore, keeping in mind the lack of research work, this work has been focussed on Lunglei and the surrounding areas which is the southern segment of Surma Basin.

Sediment frequently retains information about its origins, weathering and paleoclimate conditions, tectonic configuration, varied sediment hydrodynamic circumstances, depositional environment, etc. The petrographical study is useful to constrain the provenance<sup>(4,5)</sup>, tectonic settings<sup>(6,7)</sup>, paleoclimatic conditions<sup>(8,9)</sup>, weathering factors, and the depositional environment<sup>(10)</sup> can all be constrained with the aid of a detailed petrographic analysis.

Throughout the deposition, burial, and uplift cycle of basin history, the diagenesis processes are active as the temperature, pressure, and chemical changes of the ambient environment. Diagenesis, therefore, covers a wide range of post-depositional alterations to sediments. Because the volume and distribution of porosity in sandstones regulate hydrocarbon migration paths in the subsurface and, ultimately, the production of oil and gas from reservoirs, the petroleum industry serves as a good example of the significance of sandstone diagenesis as a subject<sup>(11,12)</sup>. The purpose of this work is to use petrography to comprehend the origin, tectonic settings, depositional environment, paleoclimatic conditions, and diagenetic events of the Bhuban sandstone in and around Lunglei, Mizoram.

## 2 Methodology

The research area is in and around Lunglei town, which is around 170 kilometers from Aizawl, Mizoram's capital. It is covered by Survey of India Toposheet Nos 84B/9 and 84B/13 and is located between 22° 45'0"N and 23° 0'0"N, with longitudes ranging from 92° 20'30"E to 92° 51'30"E. The research area's location map is shown in Figure 1. Lunglei, the district capital of Lunglei district, is located in the south-central region of Mizoram. According to the litho-stratigraphic sequence of Mizoram<sup>(13)</sup>, Lunglei town,

and its surroundings come within the Surma group of rocks. The litho-stratigraphic succession of Mizoram is presented in Figure 2.

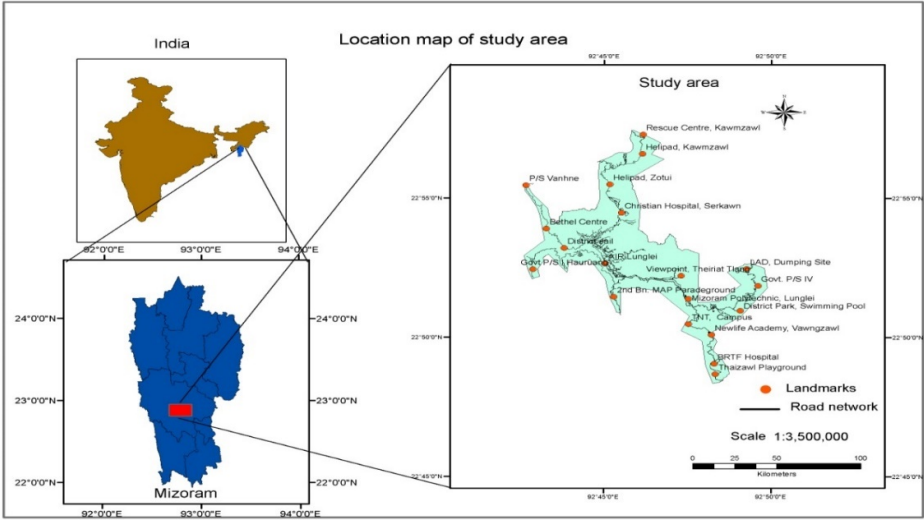


Fig 1. Location map of the study area

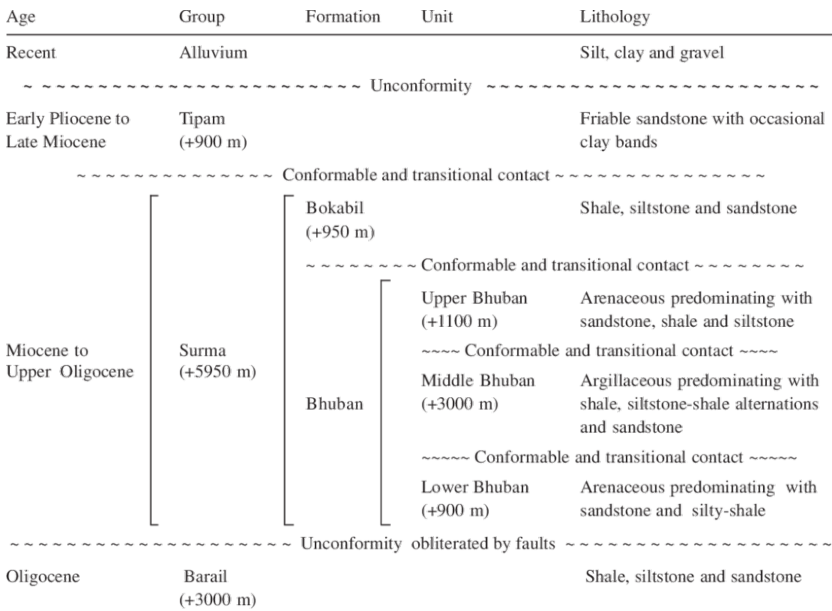


Fig 2. Litho-stratigraphic Succession of Mizoram<sup>(13)</sup>.

Thirty-seven typical Bhuban rock samples were gathered during geological fieldwork in and around the town of Lunglei. At RGL-ONGC, Sivasagar, Assam, these rock samples from the Bhuban formation in and around Lunglei town region were sent for thin section processing. Leica DME2700 P petrological magnifying tool equipped with Leica DFC420 camera, Leica picture examination computer program (LAS-v4.6), and the Department of Geology at Mizoram University was used to conduct the modular investigation, which involved checking 400 focuses per thin section according to the Gazzi-Dickinson point<sup>(14)</sup> checking strategy. To determine the provenance and tectonic settings of the study area, various plotting techniques were applied to the quantified framework mineral compositions.

### 3 Results and Discussion

#### 3.1 Petrography

The Bhuban sandstones are large, with medium to fine-grained, moderately to highly sorted sandstones. The majority of the framework grains, or 65.99% of them, were quartz grains, which are also the most prevalent detrital elements. Additionally, lithic fragments (on average 7.75%), feldspars (1.89%), and micas (on average 4.59%) were discovered. Generally monocrystalline in nature, quartz has a form that ranges from sub-angular to sub-rounded, while polycrystalline variants are also present. Although most monocrystalline types are not undulatory, some of them are currently exhibiting undulatory extinction. Both variants of 2-3 and >3 grains per quartz have poly-crystalline structures. Straight connections are what distinguish quartz from other materials, however, point and suture contact boundaries are also present. In addition to metamorphic rocks, plutonic rocks are a major source of polycrystalline quartz. The 2-3 crystal unit per grain variety (avg. 1.60%) outnumbers the >3 crystal unit per grain variety (avg. 0.64%) among polycrystalline types. There are also authigenic quartz variations and overgrowth. A few portions show the floating nature of the framework grains within the cement or matrix. 1.89 percent of all the framework grains were feldspar. Plagioclases are not as prevalent as K-feldspars. Perthite (intergrowth between plagioclase and K-feldspars) and altered feldspar (to sericite) grains can be seen in some parts.

Both allogenic and authigenic phyllosilicates are frequently found in nature. Due to their greater resistance to chemical change, muscovites are more common than biotite. The majority of authentic variations of mica come from argillaceous cement and matrix, which shows a late stage of diagenesis. Few grains are bent and fill the space between the grains of the framework. Chlorites are also infrequently seen. Among the clay minerals, kaolinite was found as tiny, mosaic-like aggregates of crystals, frequently taking the place of feldspar in the spaces between detrital grains.

In general, matrix, which makes up 9.41% of the total binding material, is produced during diagenesis by altering the framework grains or as a result of clay minerals precipitating. In a few thin layers, cementing elements such as silica, clay minerals, and carbonates are also visible. Petrographic information is provided in Table 1.

**Table 1. Modal count of petrographic study of thin sections (where, Q<sub>Mu</sub>: Monocrystalline undulatory quartz, Q<sub>Mnu</sub>: Monocrystalline non-undulatory quartz, Q<sub>P2-3</sub>: Polycrystalline quartz with 2-3 grains per quartz, Q<sub>P>3</sub>: Polycrystalline quartz with >3 grains per quartz, P<sub>Ca/Na</sub>: Plagioclase, F<sub>K</sub>: Potash feldspar, RF<sub>Ig</sub>: Igneous rock fragment, RF<sub>Sed</sub>: Sedimentary rock fragment, RF<sub>Met</sub>: Metamorphic rock fragment, C<sub>Sil</sub>: Siliceous cement, C<sub>Arg</sub>: Argillaceous cement, C<sub>Fer</sub>: Ferruginous cement, C<sub>Cal</sub>: Carbonate cement.**

Sample No.	Quartz				Feldspar		Rock Fragments			Cement				Mica	Matrix
	Q <sub>Mu</sub>	Q <sub>Mnu</sub>	Q <sub>P2-3</sub>	Q <sub>P&gt;3</sub>	P <sub>Ca/Na</sub>	F <sub>K</sub>	RF <sub>Ig</sub>	RF <sub>Sed</sub>	RF <sub>Met</sub>	C <sub>Sil</sub>	C <sub>Arg</sub>	C <sub>Fer</sub>	C <sub>Cal</sub>		
LS-1	3.8	66.03	0.2	0	0.5	0	3	6.8	1.44	0	7.43	0	0	6.4	7.1
LS-2	2.6	57.14	3.7	0.5	0.8	0.7	1.2	4.9	3.7	0	3.77	2.69	0	5.8	12.5
LS-3	5.4	66.61	0.9	0	0.9	0.9	0.1	7.2	0.3	0	7.39	0	0	6.1	4.2
LS-4	2.9	54.15	0.6	0	0.3	0.9	0	6.9	2.6	0	3.59	4.76	0	7.2	16.1
LS-5	63	61.36	1.3	2	0	0.2	2	6.4	1.7	0	7.44	0	0	6	8.9
LS-6	3.1	64.73	2.9	13	0.7	2.3	0	2.5	0.2	0	11.05	0	7.92	3.3	0
LS-7	3.6	65.11	0.2	0	0.5	0.5	0	7.6	0.3	0	3.83	6.11	0	5.6	6.65
LS-8	4.5	66.21	0.5	0	0.5	0.5	0.4	4.1	11	0	1022	3.29	0	63	2.38
LS-9	3.5	57.05	0.7	0	0.5	0	0.5	7.3	0	0	4	0	9.65	5.5	11.3
LS-10	6.6	52.28	1.5	0.2	0.5	0.9	0.7	5.1	2.3	0	1233	0	0	6.6	10.99
LS-11	4	53.75	0.5	0	0	0	0	4.2	3.4	0	9.55	0	0	8.7	15.9
LS-12	1.4	62.06	0.8	0	0	0	0	3.4	1.6	0	10	1.44	0	4.2	15.1
LS-13	2.7	63.39	2.5	5	1.2	0.2	0.6	5.8	0	7.99	5.29	0	0	3	6.83
LS-14	3.1	65.21	1.8	0.5	0.5	0	0.2	9.8	2.4	0	633	1.57	0	3.3	5.29
LS-15	1.7	66.11	1.4	0.2	0	0	0	8.6	1.2	0	0	6.29	0	0.5	14
LS-16	3.6	65.42	2.1	0.7	0	0.7	0.1	10.6	2.8	0	4.77	0.84	0	4.6	3.77
LS-17	3.89	62.18	2.33	1.55	0.52	0	0.3	6.1	2.2	0	0	5.55	0	3.5	11.88
LS-18	25	59.36	3.3	0.8	0.2	3.8	0.4	1.3	0.5	0.97	8.37	0	0	0.5	18
LS-19	2.3	63.84	1.3	1.8	0.7	15	2	9.6	13	0.77	6.15	0	0	1.3	9.24
LS-20	7.3	61.08	2.4	0.2	0.5	4.3	0	6.5	2.6	0	7.23	0	0	2.1	5.79
LS-21	2	65.24	0.7	0.7	0.7	0.7	0.6	9.6	2.3	5.19	4.8	0	0	4.7	2.77
LS-22	2.1	64.45	1.8	0.5	0.5	3.1	0.2	5.7	3.1	0	0	0	0	1	17.55
LS-23	11.5	52.82	3.2	1	1.2	2.5	0	2.2	1.1	0	9.33	0	4.76	1.2	9.19
LS-24	2	53.72	2	23	0.5	1	0	3.4	1.2	10.73	6.11	0	0	5.6	11.44

Continued on next page

Table 1 continued

LS-25	5.2	55.28	0.5	0	0.5	0	0	5.6	0.2	4.34	7.61	0	0	114	9.37
LS-26	4.1	59.39	1.3	0	1.6	6.5	3	9.2	0.8	0	4.96	0	3.81	0.8	7.24
LS-27	6.1	52.08	0.5	0	0.8	2.7	0	1.2	0.3	0	0	0	18.32	18	0
LS-28	6.1	52.53	3.4	2.3	0.5	5.2	0	1.3	0.6	1.98	10.03	0	0	4.4	11.66
LS-29	10.3	55.14	1.3	0.5	0.5	3.4	0.4	5.6	1.5	5.82	7.77	0	0	0.2	7.57
LS-30	6.5	52.48	1.7	0	0.5	0.7	0	5.8	0.3	0	11.52	0	0	2.2	18.3
LS-31	6.9	55.46	1.1	0.2	0.2	4.6	0.3	8.3	2.4	0	3.54	0	0	1.1	15.9
LS-32	10.6	50.21	25	19	0.6	1.2	0	6.8	2.4	0	10.46	0	0	7.4	5.93
LS-33	2.1	58.66	1	0.2	0.5	0.2	0	9.5	3.1	0	7.5	3.73	0	6.4	7.11
LS-34	15.4	54.1	2.4	5.1	0.3	0.3	0	3.8	3	0	0	0	15	0.6	0
LS-35	3.8	53.46	3	0.5	0.7	1	0	2.6	5.66	0	7.21	3.44	4.13	2.9	11.6
LS-36	9.4	53.06	1.1	0	0	0	0.3	4.1	0.8	0	7.23	0	0	6.6	17.41
LS-37	4	54.47	1	0.2	0.5	0.7	0	8.3	1.4	0	9.57	0	5.21	5.1	9.55

## 3.2 Depositional Environment

### 3.2.1 Sandstone Classification

Sandstones are frequently categorized using data from petrographic quantitative modal analysis<sup>(15,16)</sup>. The Bhuban sandstones' modal analysis reveals that quartz (avg. 65.99%) predominates, followed by rock fragments (avg. 7.75%) and feldspar (avg. 1.89%). In the ternary plot of QFL after Pettijohn<sup>(15)</sup>, and the ternary plot of QFR after Folk<sup>(16)</sup>, the recalculated percentile values of quartz, feldspar, and rock pieces are displayed. According to the ternary plot of the QFL, the majority of the Bhuban samples are clustered in the field of sublitharenite, while only a small number are plotted in the field of subarkose, as shown in Figure 3A. The samples are also grouped together in the field of sublitharenite seen in Figure 3B of the QFR ternary plot that follows Folk<sup>(16)</sup>. Bhuban sandstones are therefore of the sublitharenite and subarkose types.

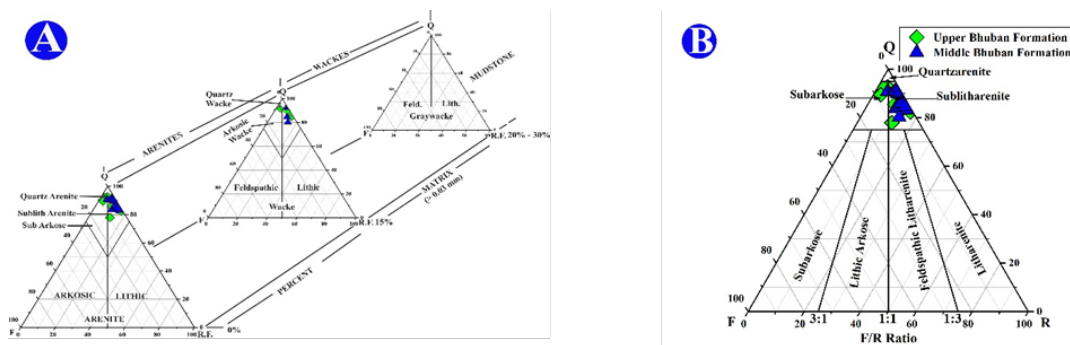


Fig 3. Petrographic classification of sandstones: A. QFL<sup>(15)</sup> and B. QFR<sup>(16)</sup>

### 3.2.2 Provenance

The nature and variations of the framework grains are frequently used to infer the provenance of the clastic sediment, which is regarded as a highly important component of a basin study. Quantitative data of polycrystalline (2-3 grains and >3 grains per quartz) and monocrystalline (both undulatory and non-undulatory) variations of quartz are frequently used to determine the composition of the source rocks. Petrographical modal data indicate that  $Q_{Mnu}$  (58.81%) dominates, with  $Q_{Mu}$  (4.94%),  $Q_{P2-3}$  (1.60%), and  $Q_{P>3}$  (0.64%) following closely behind. In order to determine the provenance, Basu *et al.*<sup>(17)</sup> presented the diamond diagram based on modal data. The Bhuban sandstones are included in the plutonic and intermediate and upper-rank metamorphic rocks when plotted in the diamond diagram (Figure 4A). The presence of sediments from plutonic and metamorphic terrains is indicated by this observation. By using the same diamond diagram settings and adding new fields of source rocks, Tortosa *et al.*<sup>(18)</sup> developed a different provenance plot. Most of the samples are in the center of this plot (Figure 4B), which shows that non-undulatory monocrystalline quartz predominates over polycrystalline quartz. As a result, it can be assumed that the granitic terrain was where the majority of the sediments came from. These discriminating plottings suggest that the granitoid and middle to upper-rank metamorphics were the likely sources of the sediments' felsic nature origin.

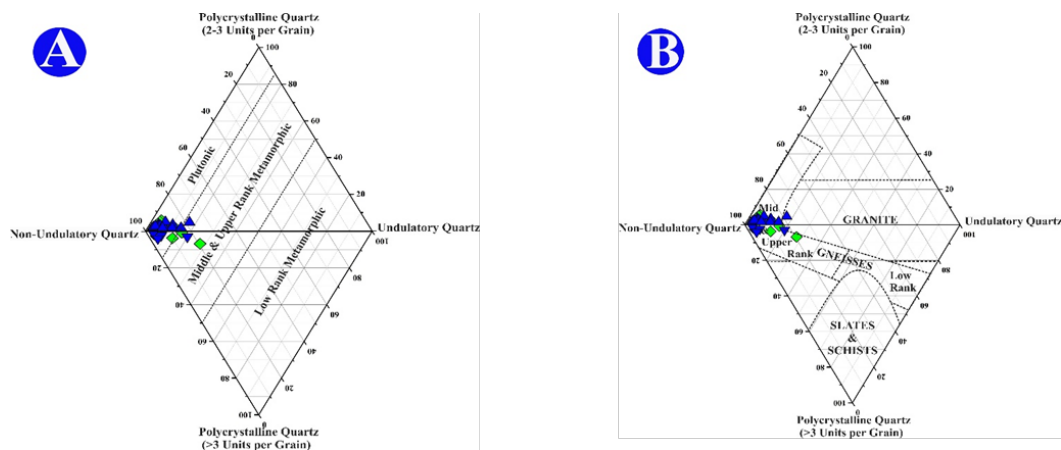


Fig 4. Monocrystalline and polycrystalline quartz are plotted as follows: A. A diamond plot after Basu *et al.*,<sup>(17)</sup> represents the derivation of sediments from plutonic and upper to middle-rank metamorphic rocks; B. A diamond plot after Tortosa *et al.*,<sup>(18)</sup> represents the derivation of sediments from granite and gneiss

### 3.2.3 Maturity

In order to show the origin of sediments as well as the level of maturity developed during transportation, Dickinson *et al.*<sup>(19)</sup> devised the ternary plot of  $Q_mPK$ . According to Figure 5, the analyzed sandstone samples exhibit a mature character with an increasing quartz concentration as a result of moderate to long-distance transportation. It shows how the sediments came to be as a result of continental block provenance weathering. In addition, a modal count of petrographic data indicates that feldspar enrichment is less than average ( $P_{Ca/Na}$ : 0.51% and  $F_K$ : 1.38%), which suggests that the sediments may have been transported moderately too far away or reworked.

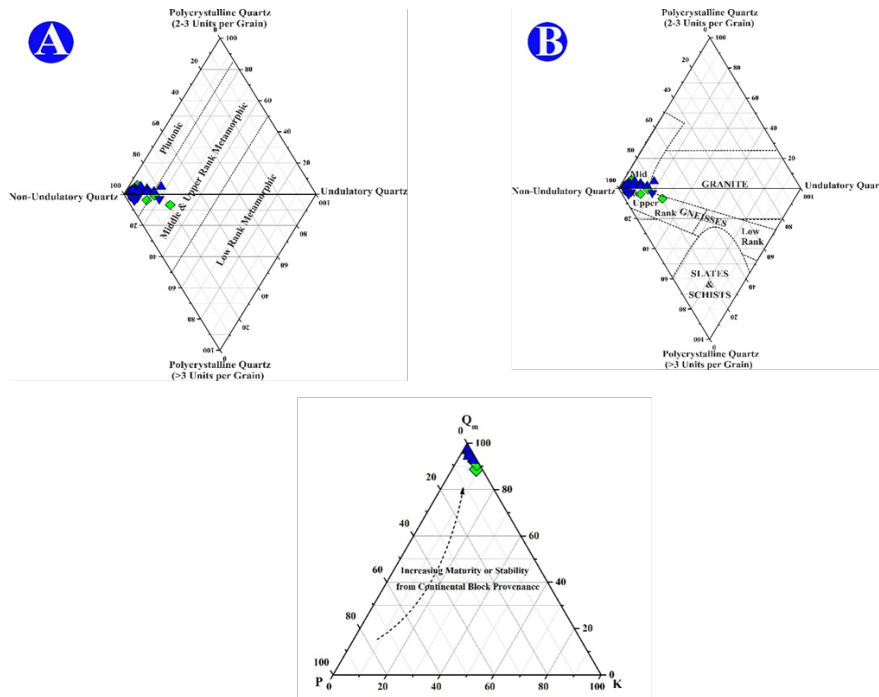


Fig 5.  $Q_mPK$  ternary plot<sup>(19)</sup> representing continental derivation of sediments with increasing maturity index



### 3.2.4 Paleo-environment

The modal count of petrographic data offers crucial hints to deducing the climate that prevailed during the period of sediment deposition in a basin. According to Suttner and Basu<sup>(20)</sup>, the bivariate plot of QFR shows that sediments were derived from a metamorphic source area under humid climatic conditions because of the high abundance of quartz and a very small amount of feldspar (Figure 6A). When combined with a bivariate plot of  $\ln(Q/R)$  vs  $\ln(Q/F)$  following Weltje<sup>(21)</sup>, (Figure 6C), Grantham and Velbel<sup>(22)</sup> proposed weathering index  $WI=C \times R$  (WI-Weathering index, C-Climate, and R-Relief) can effectively depict the nature of paleoclimatic conditions. With weathering indices between 1-2 and mixed metamorphic and plutonic rock characteristics, the Bhuban sandstones in that plot indicate moderate weathering under humid to sub-humid climatic conditions. Suttner and Dutta<sup>(7)</sup> bivariate plot of the ratios of  $(Q_{Total}/F+RF)$  vs.  $Q_P/F+RF$ , which shows that samples are grouped between semi-humid and humid climatic conditions, supports a similar interpretation (Figure 6B).

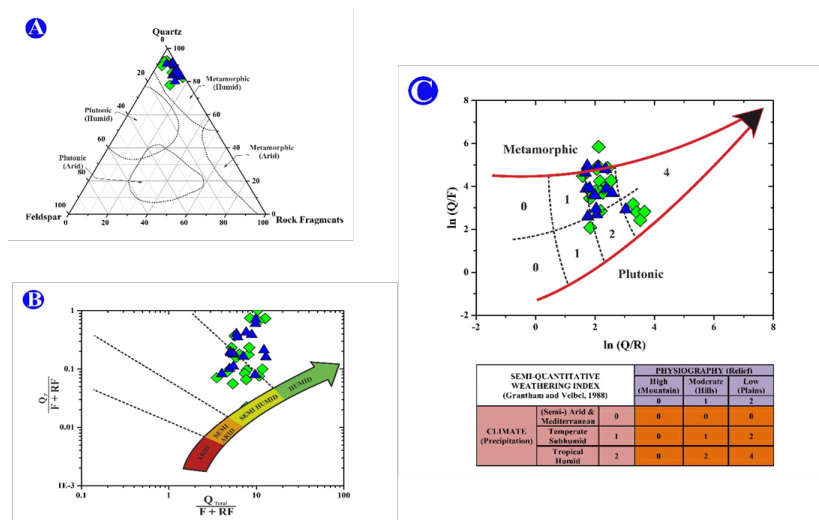


Fig 6. Paleo-climatic conditions of Bhuban Formation – A. Ternary QFR plot<sup>(20)</sup> representing humid climatic conditions. B. Bivariate plot<sup>(23)</sup> of modal data representing humid to semihumid climatic conditions. C. Semi-Quantitative Weathering Index<sup>(22)</sup> and binary plot of  $\ln(Q/R)$  vs  $\ln(Q/F)$ <sup>(23)</sup> representing moderate nature of weathering

### 3.2.5 Tectonic setting

Petrographic modal data are shown in the ternary plot of QFL after Dickinson & Suczek<sup>(24)</sup> (Figure 7A) and the ternary plot of  $Q_mFL_t$  after Dickinson et al.,<sup>(25)</sup> to ascertain the tectonic settings of the study area (Figure 7B). The plots depict an internal craton, a recycled orogen, and a recycled quartzose environment, respectively. Additionally, the tectonic configuration of the research area indicates that it is situated close to the convergent plate edge between the Indian and Burmese plates. Therefore, it may be claimed that the current study area belongs to the active continental margin to recycle the orogen transition zone.

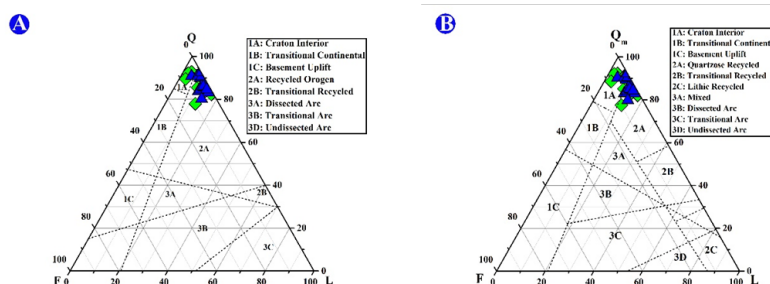


Fig 7. Petrographic tectonic setting discriminant plot– A. QFL ternary plot<sup>(24)</sup> and B.  $Q_mFL_t$  ternary plot<sup>(25)</sup> representing craton interior and quartzose recycled orogeny

### 3.2.6 Diagenesis

**Compaction:** In the current investigation, straight or long contact is frequently observed (Figure 8a). However, concavo-convex contact (Figure 8 a) and suture contact are also observed at places. In some slides, feldspar grains embaying detrital micas forming concavo-convex contact is common. Concavo-convex contact has been established between adjacent micaceous grains i.e., quartz and feldspar grains. The mica grains and ductile clay minerals were driven into the nearby pore spaces by compaction. In most of the samples of the present study, it has been observed that micas are orienting more or less in the same direction. At places, mechanical compaction is taken over by chemical compaction processes as suggested by suture contact between quartz grain which is observed locally. Undulose quartz with concavo-convex contact is occasionally observed, which may be attributed to external stresses rather than the optical characteristics retained from the source rock.

**Cementation:** In some samples of Bhuban sandstones of Lunglei, silica cement occurred in the form of overgrowths in monocrystalline quartz (Figure 7d). Most sections lack the immediately visible "dust rims" that mark the boundaries of the original detrital quartz crystal, and the quartz overgrowth is sometimes difficult to recognize under a microscope. Among the clay cement, kaolinite is commonly observed which occurs as intermixing with other clay minerals (Figure 8 c).

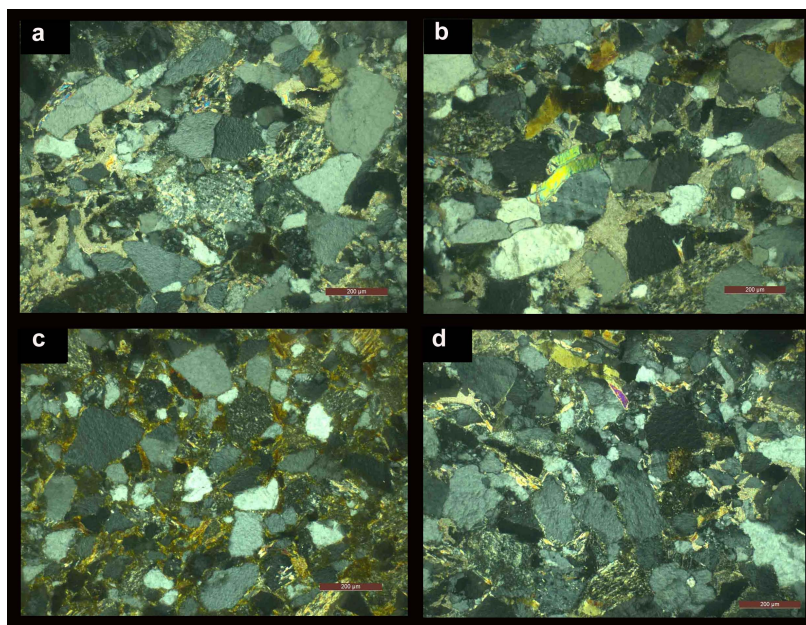


Fig 8. Photomicrograph of Bhuban Sandstone in and around Lunglei under crossed Polarized light (XPL). a: Partial replacement of Plagioclase grain (center). Poikilotopic calcite cement enclosing a number of quartz fragments (At the left side of the photo). Straight/long contact and concavo-convex contact between quartz grains are also seen. b: Deformed mica conforming with the grain boundary of detrital quartz grain. c: Clay minerals fill pore spaces that act as cementing materials. d: Quartz overgrowths filling pore spaces resulting in the interlocking of quartz grains

The frequent presence of feldspar grain in the majority of the section suggests that kaolinite is connected to the alteration of unstable feldspar. Chlorite cement is also observed in some slides showing greenish color under plane-polarized light. It is common to identify that carbonate cement as the main cementing material in the Bhuban sandstones of Lunglei. Some sections show carbonate mud filling pore spaces. There are also instances of poikilotopic calcite cement encasing some detrital grains like quartz, feldspar, and other rock fragments.

**Dissolution and Replacement:** Most of the dissolution seen in the Bhuban sandstones of Lunglei are detrital K-feldspar and Plagioclase. Although the partial dissolution of microcline and plagioclase is frequently seen, complete dissolution is not common. The subsequent precipitation of cement fills the pore space left by the dissolution. The majority of the observed alterations in the area under study are the partial replacement of the host grains, primarily plagioclase and K-feldspar grains by clays minerals. Partial alterations of the detrital feldspar grain by sericite scattering in the host grain are common.

Long and straight contacts are common in moderate compaction, while concavo-convex contacts become more prevalent with an increase in compaction and substantial grain deformation, and sutured (pressure-solution) contacts predominate with extensive compaction<sup>(26)</sup>. In the current investigation, straight or long contact and concavo-convex contact are frequently observed. While suture contact is rare although it is observed locally. As a result of compaction, ductile shale clast has flowed



into the pore space nearby thereby forming the pseudo matrix while also removing the primary porosity that was initially present in the sedimentary deposit<sup>(27)</sup>. Folded or bending mica grains are frequently seen in the Bhuban sandstone of Lunglei. It is likely that mechanical compaction caused the bending of mica grains and embaying by detrital minerals. Moreover, some section shows that micaceous grains align themselves which is probably in a direction perpendicular to the lithostatic pressure during compaction. Based on the petrographical evidence, compaction and deformation dominate the paragenetic sequence of the Bhuban sandstone of Lunglei.

Overgrowths are more likely to be found in non-undulatory monocrystalline quartz grains than in undulose or polycrystalline grains<sup>(28)</sup>. In some samples of Bhuban sandstones of Lunglei, silica cement is the most commonly observed cementing material which occurred in the form of overgrowths in monocrystalline quartz. During mesogenic burial at a temperature above 60° – 80° C, with a maximum temperature of 90° -165°, quartz overgrowths are commonly formed<sup>(29)</sup>. Clay coatings of detrital quartz and feldspar are very common in most of the samples which are likely inherited<sup>(30)</sup> or to have formed soon after the sediment was deposited by the infiltration of muddy fluids. Clays that have undergone a pseudomorphic or neomorphic transformation often reduce porosity and permeability and raise the risk of formation damage in sandstone reservoirs, which can have a substantial impact. Most of the authigenic clays identified in the Bhuban sandstone of Lunglei exhibit characteristic pore-filling or grain-coating patterns and occurred in the form of pore linings or pore-fillings and pseudomorphic replacements. Carbonate cement can be formed in all stages of diagenesis<sup>(31)</sup>. It has been observed that carbonate is the main cementing material in Bhuban sandstones of Lunglei. Poikilotopic calcite cement enclosing some detrital grains like quartz, feldspar, and other rock fragments is commonly observed.

The detrital minerals K-feldspar and calcic plagioclase feldspar are among the most prominent ones that frequently dissolve<sup>(32)</sup>. In Bhuban sandstones of Lunglei, most of the dissolution observed is in detrital K-feldspar and Plagioclase. Complete dissolution is rare; however, partial dissolution of microcline and Plagioclase is commonly observed. It is difficult to determine whether the dissolution is caused by dewatering due to compaction or due to fluid flow in the sedimentary basin. The detrital feldspar is not uniform when they are incorporated into the sediments. They are characterized by zoning and twinning which are highly susceptible to replacement<sup>(32)</sup>. Alterations observed in the present study area are mostly partial alterations of the host grain mainly plagioclase and K-feldspar by clays and calcite minerals. In some sections, specific zones or twin lines in the original feldspar grain which are more susceptible to alterations were selectively attacked by clay minerals.

## 4 Conclusion

Based on various petrographic observations, the majority of the Bhuban sandstones in and around Lunglei town are sublitharenite and sub-arkose types. The main source of sediments in the research area came from granitoid and their metamorphic counterparts, which were transported by the paleo-Bramaputra and its tributaries and created a deltaic environment. Sediments are deposited under shallow marine to deltaic conditions due to the alternate event of sea transgression and regression. Additionally, some sediments probably came from areas close to most orogens, such as the Shillong plateau, the Naga Hills, and the Indo-Burmese Ranges.

Before the occurrence of the deposition, the originating sediments underwent mild to moderate weathering under semi-humid to humid climatic conditions. The sediments had a fair amount of maturity.

The examined Bhuban sandstone has an active continental edge to the craton interior and recycled orogen setting, which supports regional tectonic configuration even if it is challenging to deduce the tectonic settings only based on the petrographic investigation.

Based on the petrographical evidence, compaction and deformation dominate the paragenetic sequence of the Bhuban sandstone of Lunglei. Quartz and silica are the main cementing materials that likely form during all stages of diagenesis. Clay coatings are common which obstruct the pores and reduce the permeability.

## 5 Declaration

Presented in 4<sup>th</sup> Mizoram Science Congress (MSC 2022) during 20<sup>th</sup> & 21<sup>st</sup> October 2022, organized by Mizoram Science, Technology and Innovation Council (MISTIC), Directorate of Science and Technology (DST) Mizoram, Govt. of Mizoram in collaboration with science NGOs in Mizoram such as Mizo Academy of Sciences (MAS), Mizoram Science Society (MSS), Science Teachers' Association, Mizoram (STAM), Geological Society of Mizoram (GSM), Mizoram Mathematics Society (MMS), Biodiversity and Nature Conservation Network (BIOCON) and Mizoram Information & Technology Society (MITS). The Organizers claim the peer review responsibility.

## References

- 1) Lalmuankimi C, Kumar S, Tiwari RP. Geochemical study of upper Bhuvan sandstone in Muthi, Mizoram, India. *Science Vision*. 2011;11(1):40–46. Available from: <https://www.sciencevision.org/storage/journal-articles/February2019/WS7bu3QDbhzShEjPE0xD.pdf>.
- 2) Lalnunmawia J, Lalhlipuii J. Classification and provenance studies of the sandstones exposed along Durtlang road section, Aizawl, Mizoram. *Science Vision*. 2014;14(3):158–167. Available from: <https://www.sciencevision.org/storage/journal-articles/February2019/Aa9BXddQZuwdzMjdtfy.pdf>.
- 3) Bubul B. A Study On Tectono Provenance And Depositional Environment Of The Bhuvan Formation In And Around Aizawl Mizoram. 2018. Available from: <http://hdl.handle.net/10603/250505>.
- 4) Augustsson C. Influencing Factors on Petrography Interpretations in Provenance Research—A Case-Study Review. *Geosciences*. 2021;11(5):1–25. Available from: <https://doi.org/10.3390/geosciences11050205>.
- 5) Shrivastava S, Singh V, Usmani HU. Petrographic classification and Provenance study of Bhandar Sandstones of the Vindhyan Supergroup, in the N-W Part of Bhopal, Madhya Pradesh, India. *Journal of Science and Technology*. 2021;6(5):111–121. Available from: <https://jst.org.in/admin/uploads/JST060524.pdf>.
- 6) Makulana M, Baiyegunhi C, Masango S. Petrography, modal composition, and tectonic provenance of some selected sandstones from the Swaershoek and Alma Formations (Waterberg Group) and Glentig Formation, Limpopo Province, South Africa: evidence from framework grains. *Arabian Journal of Geosciences*. 2022;15(697). Available from: <https://doi.org/10.1007/s12517-022-09989-1>.
- 7) Baiyegunhi TL, Liu K, Gwavava O, Baiyegunhi C. Petrography and Tectonic Provenance of the Cretaceous Sandstones of the Bredasdorp Basin, off the South Coast of South Africa: Evidence from Framework Grain Modes. *Geosciences*. 2020;10(9):1–22. Available from: <https://www.mdpi.com/2076-3263/10/9/340>.
- 8) de Cisneros CJ, González-Ramón A, Sequero C, Andreo B, Fairchild IJ. Isotopic and Petrographic Evidence as a Proxy in Paleoclimatic Reconstructions from Flowstones in Southern Spain. *Open Journal of Geology*. 2020;10(6):597–611. Available from: <https://doi.org/10.4236/ojg.2020.106027>.
- 9) Kumar A, Singh AK, Paul D, Kumar A. Paleoenvironmental, paleovegetational, and paleoclimatic changes during Paleogene lignite formation in Rajasthan, India. *Arabian Journal of Geosciences*. 2021;14(2350). Available from: <https://doi.org/10.1007/s12517-021-08638-3>.
- 10) Roy A, Chakrabarti G, Shome D. Neoproterozoic sedimentation and depositional environment: an example from Narji Formation, Cuddapah Basin, India. *Journal of Sedimentary Environments*. 2020;5:559–574. Available from: <https://doi.org/10.1007/s43217-020-00035-2>.
- 11) Burley SD, Worden RH. Sandstone diagenesis: Recent and Ancient. Blackwell Publishing Ltd. 2003.
- 12) Lawan AY, Worden RH, Utley JEP, Crowley SF. Sedimentological and diagenetic controls on the reservoir quality of marginal marine sandstones buried to moderate depths and temperatures: Brent Province, UK North Sea. *Marine and Petroleum Geology*. 2021;128:104993–104993. Available from: <https://doi.org/10.1016/j.marpetgeo.2021.104993>.
- 13) Karunakaran C. Geology and mineral resources of the states of India. Miscellaneous publication (Geological Survey of India). 1974.
- 14) Dickinson WR. Interpreting detrital modes of greywacke and arkose. *Journal of Sedimentary Petrology*. 1970;40(2):695–707. Available from: <https://gsi.ir/Images/Amozesh/Detrital%20modes-Dickinson%201970.pdf>.
- 15) Pettijohn FJ, Potter PE, Siever R. Sand and Sandstones. 1st ed. Springer Study Edition; New York, USA. Springer-Verlag. 1972. Available from: <https://doi.org/10.1007/978-1-4615-9974-6>.
- 16) Folk RL. Petrology of Sedimentary Rocks. Austin, Texas, USA. Hemphill Publishing Company. 1974.
- 17) Basu A, Young SW, Suttner LJ, James WC, Mack GH. Re-evaluation of the use of undulatory extinction and polycrystallinity in detrital quartz for provenance interpretation. *Journal of Sedimentary Research*. 1975;45(4):873–882. Available from: <https://doi.org/10.1306/212F6E6F-2B24-11D7-8648000102C1865D>.
- 18) Tortosa A, Palomares M, Arribas J. Quartz grain types in Holocene deposits from the Spanish Central System: some problems in provenance analysis. *Journal of Sedimentary Research*. 1991;57:47–54. Available from: <https://doi.org/10.1144/GSL.SP.1991.057.01.05>.
- 19) Dickinson WR, Beard L, Brakenridge GR, Erjavec JL, Ferguson RC, Inman KE, et al. Provenance of North American Phanerozoic sandstones in relation to tectonic setting. *Geological Society of America Bulletin*. 1983;94(2):222–235. Available from: [https://doi.org/10.1130/0016-7606\(1983\)94<222:PONAPS>2.0.CO;2](https://doi.org/10.1130/0016-7606(1983)94<222:PONAPS>2.0.CO;2).
- 20) Suttner LJ, Basu A, Mack GH. Climate and the origin of quartz arenites. *Journal of Sedimentary Research*. 1981;51(4):1235–1246. Available from: <https://doi.org/10.1016/j.marpetgeo.2022.106073>.
- 21) Weltje GJ. Provenance and Dispersal of Sand-sized Sediments: Reconstruction of Dispersal Patterns and Sources of Sand-sized Sediments by Means of Inverse Modelling Techniques. 1994.
- 22) Grantham JH, Velbel MA. The influence of climate and topography on rock fragment abundance in modern fluvial sands of the southern Blue Ridges mountains, North Carolina. *Journal of Sedimentary Research (SEPM)*. 1988;58(2):219–227. Available from: <https://archives.datapages.com/data/sepm/journals/v55-58/data/058/058002/0219.htm>.
- 23) Suttner LJ, Dutta PK. Alluvial sandstone composition and paleoclimate, framework mineralogy. *Journal of Sedimentary Research*. 1986;56(3):329–345. Available from: <https://doi.org/10.1306/212F8909-2B24-11D7-8648000102C1865D>.
- 24) Dickinson WR, Suczek CA. Plate tectonics and sandstone compositions. *AAPG Bulletin*. 1979;63(12):2164–2182. Available from: <https://archives.datapages.com/data/bulletins/1977-79/data/pg/0063/0012/2150/2164.htm>.
- 25) Dickinson WR, Beard L, Brakenridge GR, Erjavec JL, Ferguson RC, Inman KE, et al. Provenance of North American Phanerozoic sandstones in relation to tectonic setting. *Geological Society of America Bulletin*. 1983;94(2):222–235. Available from: [https://doi.org/10.1130/0016-7606\(1983\)94<222:PONAPS>2.0.CO;2](https://doi.org/10.1130/0016-7606(1983)94<222:PONAPS>2.0.CO;2).
- 26) Taylor JM. Pore-space reduction in sandstones. *AAPG Bulletin*. 1950;34(4):701–716. Available from: <https://doi.org/10.1306/3D933F47-16B1-11D7-8645000102C1865D>.
- 27) Monsees AC, Busch B, Hilgers C. Compaction control on diagenesis and reservoir quality development in red bed sandstones: a case study of Permian Rotliegend sandstones. *International Journal of Earth Sciences*. 2021;110:1683–1711. Available from: <https://doi.org/10.1007/s00531-021-02036-6>.
- 28) Goldstein RH, Rossi C. Recrystallization in Quartz Overgrowths. *Journal of Sedimentary Research*. 2002;72(3):432–440. Available from: <https://pubs.geoscienceworld.org/sepm/jsedres/article-abstract/72/3/432/99255/Recrystallization-in-Quartz-Overgrowths>.
- 29) Walderhaug O. Modeling Quartz Cementation and Porosity in Middle Jurassic Brent Group Sandstones of the Kvitebjørn Field, Northern North Sea. *AAPG Bulletin*. 2000;84(9):1325–1339. Available from: <https://doi.org/10.1306/A9673E96-1738-11D7-8645000102C1865D>.
- 30) Bello AM, Al-Ramadan K, Babalola LO, Alqubalee A, Amao AO. Impact of grain-coating illite in preventing quartz cementation: Example from permo-carboniferous sandstone, Central Saudi Arabia. *Marine and Petroleum Geology*. 2023;149:106073–106073. Available from: <https://doi.org/10.1016/j.marpetgeo.2022.106073>.

- 31) Liu G, Hu G, Shi X, Ma Y, Yin X, Li A. Carbonate cementation patterns and diagenetic reservoir facies of the triassic Yanchang Formation deep-water sandstone in the huangling area of the Ordos Basin, northwest China. *Journal of Petroleum Science and Engineering*. 2021;203:1–14. Available from: <https://doi.org/10.1016/j.petrol.2021.108608>.
- 32) Chowdhury AH, Noble JPA. Feldspar albitization and feldspar cementation in the Albert Formation reservoir sandstones, New Brunswick, Canada. *Marine and Petroleum Geology*. 1993;10(4):394–402. Available from: [https://doi.org/10.1016/0264-8172\(93\)90083-5](https://doi.org/10.1016/0264-8172(93)90083-5).